



Deposited via The University of Leeds.

White Rose Research Online URL for this paper:

<https://eprints.whiterose.ac.uk/id/eprint/105964/>

Version: Published Version

---

**Article:**

Artexte, M, Nahil, MA, Olazar, M et al. (2016) Steam reforming of phenol as biomass tar model compound over Ni/Al<sub>2</sub>O<sub>3</sub> catalyst. *Fuel*, 184. pp. 629-636. ISSN: 0016-2361

<https://doi.org/10.1016/j.fuel.2016.07.036>

---

**Reuse**

Items deposited in White Rose Research Online are protected by copyright, with all rights reserved unless indicated otherwise. They may be downloaded and/or printed for private study, or other acts as permitted by national copyright laws. The publisher or other rights holders may allow further reproduction and re-use of the full text version. This is indicated by the licence information on the White Rose Research Online record for the item.

**Takedown**

If you consider content in White Rose Research Online to be in breach of UK law, please notify us by emailing [eprints@whiterose.ac.uk](mailto:eprints@whiterose.ac.uk) including the URL of the record and the reason for the withdrawal request.

1     **Steam reforming of phenol as biomass tar model compound**  
2                                   **over Ni/Al<sub>2</sub>O<sub>3</sub> catalyst**

3     Maite Artetxe<sup>b</sup>, Mohamad A. Nahil<sup>a</sup>, Martin Olazar<sup>b\*</sup>, Paul T. Williams<sup>a</sup>

4             <sup>a</sup>Energy Research Institute, University of Leeds, Woodhouse lane, Leeds LS2 9JT,  
5                                   United Kingdom

6             <sup>b</sup>Department of Chemical Engineering, University of the Basque Country, P.O. Box  
7                                   644 - E48080, Bilbao, Spain

8

9                                   [martin.olazar@ehu.es](mailto:martin.olazar@ehu.es)

10                                Tel.: +34 946 012 527

11                                Fax: +34 946 013 500

12

13 **Abstract**

14 Catalytic steam reforming of phenol over Ni/Al<sub>2</sub>O<sub>3</sub> catalyst with 10 wt% of Ni loading  
15 was carried out in a fixed bed reactor. The effect of temperature (650-800 °C), reaction  
16 time (20-80 min) and catalyst amount (0-2 g corresponding to 0-4.5 g<sub>cat</sub> h g<sub>phenol</sub><sup>-1</sup>) on  
17 carbon conversion, H<sub>2</sub> potential and catalyst deactivation was studied. High efficiency  
18 of Ni/Al<sub>2</sub>O<sub>3</sub> catalyst in steam reforming of phenol is observed at 750 °C for a reaction  
19 time of 60 min when 1.5 g of catalyst (3.4 g<sub>cat</sub> h g<sub>phenol</sub><sup>-1</sup>) is used, with carbon conversion  
20 and H<sub>2</sub> potential being 81 and 59 %, respectively. An increase in temperature enhances  
21 phenol reforming reaction as well as coke gasification, minimizing its deposition over  
22 the catalyst. However, at high temperatures (800 °C) an increase in Ni crystal size is  
23 observed indicating catalyst irreversible deactivation by sintering. As catalyst time on  
24 stream is increased the coke amount deposited over the catalyst increases, but no  
25 differences in Ni crystal size are observed. An increase in catalyst amount from 0 to 1.5  
26 g increases H<sub>2</sub> potential, but no further improvement is observed above 1.5 g. It is not  
27 observed significant catalyst deactivation by coke deposition, with the coke amount  
28 deposited over the catalyst being lower than 5 % in all the runs.

29

30 **Keywords:** Ni/Al<sub>2</sub>O<sub>3</sub> catalyst, biomass gasification, tar model compound, phenol, steam  
31 reforming

32

33

## 34 **1. Introduction**

35 Biomass is considered as a potential renewable energy source in order to decrease our  
36 current dependence on fossil fuels [1,2]. Its abundance, renewability, carbon-neutrality  
37 and low sulphur content make biomass especially interesting to replace fossil fuels as  
38 energy source [3,4]. Among the different technologies, gasification is a promising one  
39 in which biomass is converted into a syngas stream that can be combusted in an internal  
40 combustion engine for power generation or in a furnace for heat generation [5,6].

41 Besides, the syngas produced can be used as a raw material for production of fuels and  
42 chemicals by Fischer-Tropsch synthesis method [7].

43 The main drawback of biomass gasification process and its large scale implementation  
44 is the formation of unwanted byproducts together with syngas, such as particulates,  
45 alkali metals, fuel-bound nitrogen, sulphur, chlorine and tar [7,8]. These byproducts  
46 cause several problems in process equipment (corrosion, clogging...) as well as  
47 environmental pollution. Tar is a complex mixture of condensable hydrocarbons with  
48 molecular weight higher than benzene and its elimination has raised significant concern  
49 in literature [3,5,8-10]. The concentration and the composition of the tar in the gas  
50 stream produced in biomass gasification depend on the raw material, the operating  
51 conditions and the gasification technology used [11]. Tar lead to several operational  
52 problems in process equipment, such as metal corrosion, clogging filters and valves or  
53 condensing in cold spots plugging them. Besides, tar concentration limits the  
54 application of the produced syngas in internal combustion engines ( $<100 \text{ mg/Nm}^3$ ) as  
55 well as gas turbines ( $<5 \text{ mg/Nm}^3$ ) due to the clogging of pipelines and injectors in  
56 engines and turbines [8]. Furthermore, tar compounds make the produced gas useless  
57 for applications such as Fischer-Tropsch process for chemical production, in which tar  
58 presence leads to serious coke deposition over the catalyst.

59 Tar removal methods can be classified in primary and secondary methods, where the  
60 gas cleaning treatment is carried out inside or downstream the gasifier respectively  
61 [10,12]. Several technologies have been studied for a downstream tar removal, generally  
62 divided into physical methods, catalytic cracking or thermal treatment [8]. Among  
63 them, downstream catalytic steam reforming is widely studied in order to convert tar  
64 compounds into useful fuel gas, thus obtaining high purity gas and increasing fuel  
65 value. Natural minerals, such as natural calcite, olivine and dolomite [13-16], nickel  
66 based catalyst [11,17,18] or non-nickel metal catalyst [4] have been extensively studied  
67 in order to find a catalyst that is inexpensive, effective in tar reduction, resistant to  
68 deactivation and easily regenerated.

69 Tar model compounds are widely used in order to deeply study the catalyst performance  
70 and the process operating conditions. Toluene, benzene, naphthalene and phenol are  
71 usually identified as the principal biomass gasification tar model compounds [3] and  
72 they are the commonly chosen tar model compounds to study its steam reforming over  
73 supported metal catalysts [4,19-22]. Ni commercial steam reforming catalyst has been  
74 widely studied for biomass tar reforming [8,11], given that it allows obtaining high tar  
75 conversion and improving the quality of the syngas, since light hydrocarbons are also  
76 reformed and higher H<sub>2</sub> yields are obtained. Besides, several supports (Al<sub>2</sub>O<sub>3</sub>, SiO<sub>2</sub>,  
77 ZrO<sub>2</sub>, MgO, olivine...) [20,23-25] and promoters (CeO<sub>2</sub>, Co, La...) [22,26] for Ni metal  
78 have been studied in the literature in order to improve the activity, stability, coking  
79 resistance and regenerability of the catalyst.

80 In this work phenol has been used as a model compound of biomass gasification tar,  
81 given that it is an oxygenated aromatic compound that is more refractory to reforming  
82 than non-aromatic compounds and causes faster deactivation than non-oxygenated  
83 compounds. Phenol steam reforming over Ni/Al<sub>2</sub>O<sub>3</sub> catalyst has been studied in order to

84 optimize the experimental conditions (temperature, reaction time, catalyst amount) for  
85 maximizing the phenol conversion and minimizing the catalyst deactivation by coke  
86 deposition as well as sintering. This study has been conducted with the aim of  
87 optimizing operating conditions for a future detailed study of the steam reforming  
88 process in which different model compounds or catalysts will be assayed. It should be  
89 noted that steam reforming of phenol over Ni metal catalyst has also been studied in  
90 order to obtain information about bio-oil steam reforming considering phenol as bio-oil  
91 model compound [27,28].

## 92 **2. Experimental**

### 93 2.1. Catalyst preparation and characterization

94 A nickel alumina catalyst (Ni/Al<sub>2</sub>O<sub>3</sub>) with a nickel loading of 10 wt.% was prepared by  
95 a simple impregnation method, and tested in the catalytic steam reforming of phenol.  
96 Approximately 11 g of nickel nitrate hexahydrate (Ni(NO<sub>3</sub>)<sub>2</sub>•6H<sub>2</sub>O, Sigma-Aldrich)  
97 were dissolved in 20 ml of deionised water and mixed with approximately 20 g of  
98 aluminium oxide (γ-Al<sub>2</sub>O<sub>3</sub>, 96% Alfa Aesar). The precursor was stirred at 100 °C for  
99 around 30 minutes to ensure homogeneous mixture of components and promote water  
100 evaporation. Subsequently, the resulting semi-solid mixture was further dried overnight  
101 at 105 °C, and calcined at 750 °C with 20 °C min<sup>-1</sup> heating rate in an air atmosphere for  
102 3 hours. The resulting catalyst was crushed and sieved to obtain finer particles with a  
103 size in the 0.18-0.24 mm range. The prepared catalyst was not reduced, since during the  
104 process some of the pyrolysis gases, such as H<sub>2</sub> and CO, have the capability to reduce  
105 the catalyst itself [29].

106 The physical or structural properties of the catalyst (BET surface area, pore volume and  
107 pore size distribution) were measured using Micromeritics TriStar 3000. These

108 properties were determined by the adsorption-desorption of N<sub>2</sub> at -192 °C. The  
109 experimental procedure consists in degassing the sample for approximately 8 h at 150  
110 °C to remove all possible impurities, followed by adsorption-desorption of N<sub>2</sub>. The  
111 surface area was calculated using the BET method and the average pore diameter was  
112 calculated using the BJH method, with the calculated values being 116.5 m<sup>2</sup>/g and 24 Å,  
113 respectively.

114 X-Ray diffraction (XRD) analyses of the catalyst were carried out using Bruker D8  
115 instrument with a CuK $\alpha$  radiation for a qualitative phase analysis (fresh catalyst) and  
116 crystal size determination (used catalyst). The samples were ground to less than 75  $\mu$ m  
117 size and loaded into the 20 mm aperture of an aluminium sample holder. Concerning the  
118 fresh catalyst, 3 different phases corresponding to NiO, Al<sub>2</sub>O<sub>3</sub> and NiAl<sub>2</sub>O<sub>4</sub> have been  
119 identified. The determinations of Ni crystal size for used catalysts were carried out  
120 using Scherrer equation.

121 Temperature programmed oxidation (TPO) of used catalysts were carried out to  
122 determine the amount and nature of the coke deposited over the catalyst for which the  
123 thermogravimetric analyzer Shimadzu TGA-50 was used. About 20 mg of sample was  
124 heated in air atmosphere at 15 °C min<sup>-1</sup> to a final temperature of 800 °C and maintained  
125 for 10 min at this temperature. Besides, high resolution scanning electron microscopy  
126 (SEM, Hitachi SU8230) was used to identify the nature of the coke deposited over the  
127 catalyst.

## 128 2.2. Experimental equipment and procedure

129 Figure 1 shows the experimental equipment used to study the steam reforming of phenol  
130 over Ni/Al<sub>2</sub>O<sub>3</sub> catalyst with 10 wt% of Ni loading. Phenol was dissolved in water at a  
131 steam/carbon molar ratio of 13, and they were fed continuously by means of a syringe  
132 pump using a flow rate of 6.64 ml min<sup>-1</sup>. The first furnace was maintained at 250 °C to

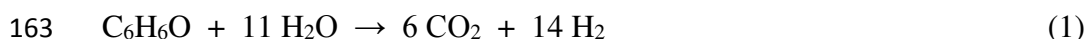
133 evaporate the feedstock before entering the second reactor. Besides, 80 ml min<sup>-1</sup> of  
134 nitrogen was fed to sweep the volatiles formed in the reactor. Both reactors were 16 cm  
135 length with an internal diameter of 2.2 cm and each was separately heated externally by  
136 an electrical furnace. The influence of the reforming reactor temperature was studied in  
137 the 650-800 °C range, using 1 g of Ni/Al<sub>2</sub>O<sub>3</sub> catalyst for a reaction time of 40 min. As  
138 aforementioned, the catalyst has not been reduced before use because H<sub>2</sub> and CO are  
139 present in the reaction medium and, as concluded in a previous work [30], they are  
140 capable of reducing the catalyst. Therefore, the effect of the reaction time (20-80 min)  
141 was studied to analyze the evolution of catalyst activity by using 1 g of Ni/Al<sub>2</sub>O<sub>3</sub> at a  
142 reforming temperature of 750 °C. Moreover, the influence of the catalyst amount on  
143 phenol conversion was analyzed in the 0-2 g range (corresponding to space-times in the  
144 0-4.5 g<sub>cat</sub> h g<sub>phenol</sub><sup>-1</sup> range) at 750 °C for 60 min.

### 145 **Figure 1**

146 The volatile stream formed goes to a condensation system which is formed by two  
147 condensers cooled with dry-ice. The non-condensable gases are collected in a 10 L  
148 Teldar<sup>TM</sup> gas sample bag. The gases are collected for 20 min subsequent to the end of  
149 each run to ensure that all the produced gases are collected. The gases collected in the  
150 gas sample bag were analysed off-line by gas chromatography. Hydrocarbon gases  
151 (from C<sub>1</sub> to C<sub>4</sub>) were determined by a Varian 3380 chromatograph with a flame  
152 ionisation detector (GC/FID), 80-100 mesh Hysep column and using nitrogen as carrier  
153 gas. Permanent gases, i.e., CO, O<sub>2</sub>, N<sub>2</sub> and H<sub>2</sub>, were determined by a Varian 3380  
154 chromatograph with a 60-80 mesh molecular sieve column and argon as carrier gas with  
155 a thermal conductivity detector, whereas CO<sub>2</sub> was analysed by another Varian 3380 GC  
156 provided with a Hysep 80-100 mesh column and using argon as carrier gas and a  
157 thermal conductivity detector.

158 The condensers were weighed before and after each run to measure the liquid amount  
159 obtained and N<sub>2</sub> was used as internal standard to calculate the gas yield. Each run was  
160 repeated at least twice to verify the reproducibility of the results and the mass balance  
161 closure was between 95-105 % in all the runs.

162 The overall reaction of catalytic steam reforming of phenol is defined as follows:



164 In order to analyze the effect of operating conditions on the steam reforming of phenol,  
165 carbon conversion and H<sub>2</sub> potential was defined. The carbon conversion was defined as  
166 the moles of carbon in the gaseous products divided by the moles of carbon fed and H<sub>2</sub>  
167 potential as percentage of the potential stoichiometric H<sub>2</sub> yield, where stoichiometric H<sub>2</sub>  
168 moles were calculated according to eq. 1.

$$169 \text{C conversion (\%)} = \frac{\text{moles of carbon in the product gas}}{\text{moles of carbon in the feed}} 100 \quad (2)$$

$$170 \text{H}_2 \text{ potential} = \frac{\text{moles of H}_2 \text{ in the product gas}}{\text{moles of H}_2 \text{ in stoichiometric potential}} 100 \quad (3)$$

171 The yield of gas compounds was calculated as follows,

$$172 \text{Yield (\%)} = \frac{\text{g of the compound in the product gas}}{\text{g of phenol fed}} 100 \quad (4)$$

### 173 **3. Results**

#### 174 3.1. Effect of temperature

175 Figure 2 shows the effect of temperature on carbon conversion and H<sub>2</sub> potential  
176 obtained in the steam reforming of phenol over Ni/Al<sub>2</sub>O<sub>3</sub> catalyst (1 g of catalyst  
177 corresponding to a space time of 2.25 g<sub>cat</sub> h g<sub>phenol</sub><sup>-1</sup>). It can be seen that temperature has

178 great influence on phenol reforming, increasing the carbon conversion from 8 % at 650  
179 °C to 57 % at 800 °C. Likewise, H<sub>2</sub> potential increases as reforming temperature is  
180 increased, reaching a value of 47 % at 800 °C. This increase in carbon conversion and  
181 H<sub>2</sub> potential can be attributed to the endothermic nature of oxygenated compound  
182 reforming reaction, which is enhanced as temperature is increased.

183

### Figure 2

184 The same trend of carbon conversion and H<sub>2</sub> yield with temperature was observed in the  
185 literature on steam reforming of phenol over Ni/Al<sub>2</sub>O<sub>3</sub> catalyst [28,31]. Wang et al. [28]  
186 studied the steam reforming of different bio-oil model compounds, in which phenol has  
187 been identified as the most refractory compound due to its stable structure with an  
188 aromatic ring.

189 Figure 3 displays the effect of temperature on the yield of the gas compounds. It can be  
190 seen that an increase in temperature increases the yield of all gas compounds due to the  
191 enhancement of reforming reaction, reaching a maximum CO<sub>2</sub>, CO and H<sub>2</sub> yield at 800  
192 °C, 66, 55 and 14 wt%, respectively. Phenol steam reforming reaction on nickel surface  
193 is explained by two possible mechanisms [32], which are initiated with the dissociation  
194 of O-H followed by: i) a ring opening caused by C-H scission and C=C rupture in  
195 positions 2 and 6; ii) C-O bond dissociation followed by C-H and C=C rupture. Both  
196 decomposition mechanisms give way to H<sub>2</sub>, CO and light hydrocarbon formation. The  
197 low values of light hydrocarbon yields obtained (lower than 1 wt% in all the  
198 temperature range studied) shows that its reforming is almost complete even at low  
199 temperatures. The low CH<sub>4</sub> yield obtained can be attributed to the absence of methyl  
200 group in the phenol structure.

201

### Figure 3

202 Nevertheless, it can be observed that the ratio between CO and CO<sub>2</sub> is significantly  
203 changed as temperature is increased, showing that an increase in temperature increases  
204 the phenol reforming reaction and causes thermodynamic equilibrium displacement in  
205 the water gas shift exothermic reaction.

206 Figure 4 shows the temperature programmed oxidation (DTG-TPO) curves for the coke  
207 deposited over Ni/Al<sub>2</sub>O<sub>3</sub> catalyst used in the steam reforming of phenol at different  
208 temperatures. Ni/Al<sub>2</sub>O<sub>3</sub> catalyst deactivation by coke deposition has been widely  
209 studied in the literature [33,34] for which two types of coke have been identified: i)  
210 amorphous coke, which is burnt at low temperatures (around 450 °C) since its  
211 combustion is activated by Ni metal on which the coke is deposited causing its  
212 encapsulation; ii) filamentous coke, which is not adsorbed over Ni sites and it is  
213 combusted at high temperatures (above 450 °C).

#### 214 **Figure 4**

215 The coke deposited over the catalyst used at 650 °C (4.6 wt%) is combusted in a wide  
216 temperature range, between 350 and 600 °C. Although a main peak at 480 °C is  
217 observed, several shoulders can be observed at different temperatures (370, 410 and 460  
218 °C), which evidence the heterogeneous nature of the coke deposited. This heterogeneity  
219 reveals the existence of nascent coke (the shoulder at 370 °C), which is formed by  
220 phenol condensation and adsorbed as phenate species over Ni sites [35] and its  
221 combustion is catalyzed by Ni metal sites. This coke evolves into more condensate  
222 structures by multilayer growing and it is separated progressively from Ni sites,  
223 requiring higher temperatures for its combustion.

224 Furthermore, the composition of the coke deposited in steam reforming depends on the  
225 operating conditions used (temperature, steam/carbon ratio and space-time) since coke  
226 deposition is a result of a balance between its formation and its elimination by

227 gasification [36]. Consequently, the coke deposited at 750 °C is significantly affected by  
228 gasification, which is faster for the less condensed coke. Thus, at 750 °C the coke  
229 amount deposited is lower (2.1 wt%) and more evolved, with the peak being moved at  
230 higher temperatures. Coke gasification rate is higher at 800 °C, decreasing the amount  
231 of coke deposited until 1.1 wt%.

232 Figure 5 shows SEM images for the fresh (a) and used catalyst (at 650 (b), 750 (c) and  
233 800 (d)). It can be seen that SEM images do not show the presence of high structured  
234 filamentous coke. It should be noted that the catalyst with the highest coke amount is  
235 that used at the lowest temperature, for which an amorphous coke deposited between  
236 catalyst particles is observed.

### 237 **Figure 5**

238 XRD analysis for the catalyst used in the reforming of phenol at 650 °C, 750 °C and 800  
239 °C have been carried out in order to study the influence of the reforming temperature on  
240 the Ni crystal size. The catalyst used at 650 °C does not present a peak representative of  
241 Ni metal, indicating that 650 °C is not high enough to reduce the catalyst. The catalyst  
242 used at 750 °C presents a peak representative of the Ni metal with a crystal size of 45 Å.  
243 Likewise, for the catalyst used at 800 °C a peak characteristic of Ni metal is observed  
244 with a crystal size of 72 Å, showing that reforming temperature causes catalyst  
245 irreversible deactivation by Ni metal sinterization.

### 246 3.2. Effect of time on stream

247 Figure 6 displays the effect of reaction time on carbon conversion and H<sub>2</sub> potential  
248 obtained in the catalytic reforming of phenol over Ni/Al<sub>2</sub>O<sub>3</sub> catalyst at 750 °C (1 g of  
249 catalyst corresponding to a space time of 2.25 g<sub>cat</sub> h g<sub>phenol</sub><sup>-1</sup>). It can be seen that an  
250 increase in time on stream until 60 min gives way to a linear increase in carbon

251 conversion, increasing from 35 % for 20 min to 56 % for 60 min. Above 60 min no  
252 change in carbon conversion is observed. As aforementioned, the catalyst is not reduced  
253 before use because H<sub>2</sub> and CO present in the reaction medium will reduce it [37]. It can  
254 be seen that an initial period of catalyst activation is necessary and the catalyst is  
255 reduced completely for the run carried out for 60 min, maintaining its activity above this  
256 reaction time. Similarly, H<sub>2</sub> potential increases as time on stream increased, reaching a  
257 maximum value of 39 % for the run carried out for 40 min and maintaining this value  
258 for longer reaction times.

### 259 **Figure 6**

260 Figure 7 shows the effect of reaction time in the catalytic reforming of phenol over  
261 Ni/Al<sub>2</sub>O<sub>3</sub> catalyst at 750 °C on the individual gas compounds yields obtained. It can be  
262 seen that an increase in reaction time until 40 min gives way to an increase in CO, CO<sub>2</sub>  
263 and H<sub>2</sub> yield (47, 58, 11 %) due to the enhancement of reforming reaction as the catalyst  
264 is reduced. An increase in reaction time from 40 to 60 min shows a significant increase  
265 in CO<sub>2</sub> yield (form 58 % to 73 %) and a slight increase in H<sub>2</sub> yield (form 11 % to 12 %).  
266 However, an increase in reaction time from 60 to 80 min gives way to a decrease in CO<sub>2</sub>  
267 (form 73 % to 63 %) and H<sub>2</sub> yield (form 12 % to 11 %), but an increase in the yield of  
268 CO (form 49 % to 57 %). The trend observed can be attributed to water gas shift  
269 reaction, which is enhanced when time on stream increases form 40 to 60 min due to the  
270 complete reduction of the catalyst and an increase in its activity. However, it seems that  
271 an increase in reaction time above 60 min reduces the catalyst activity for water gas  
272 shift reaction since coke deposition over the catalyst decrease its activity for this  
273 reaction.

### 274 **Figure 7**

275 DTG-TPO results for the Ni/Al<sub>2</sub>O<sub>3</sub> catalyst used in phenol steam reforming at 750 °C  
276 for different reaction times (Figure 8) show that the coke amount increases as reaction  
277 time is increased, from 2.1 % for 20 min to 3.8 % for 80 min. It can be seen that the  
278 coke deposited over all the catalysts studied is combusted between 350-600 °C and they  
279 present a prevailing peak around 500 °C. Nevertheless, the nature of the coke deposited  
280 over the catalyst is different depending on the reaction time. The catalyst used for 60  
281 min presents a significant shoulder at low temperatures (400 °C) and a main peak at  
282 intermediate temperatures (500 °C). Although the coke amount does not increase  
283 significantly, an increase in reaction time until 80 min gives way to a higher degree of  
284 structuring of the carbonaceous material deposited, which decreases the shoulder at low  
285 temperatures (400 °C) and increases the main peak at higher temperatures (500 °C).

### 286 **Figure 8**

287 SEM analysis for the fresh (Figure 9a) and the catalyst used for different reaction times,  
288 40 (Figure 9b), 60 (Figure 9c) and 80 min (Figure 9d), have been carried out in order to  
289 gain knowledge about the coke nature and position. Regarding the SEM images, no  
290 significant differences are observed for low times on stream due to the low coke amount  
291 deposited over the catalyst. However, for long reaction times (Figure 11d), an  
292 amorphous coke deposited is clearly observed over catalyst particles. XRD analysis has  
293 also been used to calculate the Ni crystal size and analyze the influence of the reaction  
294 time over catalyst deactivation by sintering. The catalysts used for 40, 60 and 80 min  
295 have been analyzed and no influence of reaction time over catalyst sinterization is  
296 observed, with the Ni crystal size being around 45 Å for all the catalysts studied. This  
297 evidences that there is no Ni particle dragging, which is consistent with the absence of  
298 filamentous coke.

### 299 **Figure 9**

### 300 3.3. Effect of catalyst amount

301 Figure 10 displays the effect of the catalyst amount used (0, 1, 1.5 and 2 g of catalyst  
302 corresponding to space times of 0, 2.25, 3.4 and 4.5  $\text{g}_{\text{cat}} \text{h g}_{\text{phenol}}^{-1}$ ) on carbon conversion  
303 and  $\text{H}_2$  yield obtained at 750 °C and for a reaction time of 60 min (a steam/carbon molar  
304 ratio of 13 and a flowrate of 6.64  $\text{ml min}^{-1}$ ). The run without catalyst was carried out  
305 using 1 g of sand. As observed, the catalyst used is highly efficient, given that it  
306 increases carbon conversion from 9 to 56 % and  $\text{H}_2$  yield from 4 to 38 % when 1 g of  
307 catalyst is added. An increase in the catalyst amount used from 1 to 1.5 g leads to a  
308 significant increase in carbon conversion as well as  $\text{H}_2$  potential, reaching values of 81  
309 and 59 %, respectively. However, an increase in catalyst amount above 1.5 g does not  
310 show a notable influence in phenol reforming, maintaining carbon conversion and  $\text{H}_2$   
311 yield almost constant when catalyst amount is increased to 2 g. Wang et al. [28]  
312 obtained similar results studying the steam reforming of bio-oil model compounds over  
313  $\text{Ni/Al}_2\text{O}_3$  catalyst.

### 314 **Figure 10**

315 Figure 11 shows that an increase in catalyst amount from 0 to 1.5 g gives way to a  
316 increase in the yield of  $\text{CO}$ ,  $\text{CO}_2$  and  $\text{H}_2$  from 10, 9.9 and 1.4 wt.% to 72, 111 and 17  
317 wt.%, respectively. However, an increase in space-time above this value lead to an  
318 increase in the yield of  $\text{CO}_2$  (118 wt.%) and a decrease in the yield of  $\text{CO}$  (68 wt.%),  
319 indicating that water gas shift reaction is favoured when a large amount of catalyst is  
320 used. Swierczynski et al. [38] have also seen the enhancement of water gas shift  
321 reaction when space-time is increased. They study toluene steam reforming over  
322  $\text{Ni/olivine}$  catalyst at 800 and 650 °C showing that an increase in space-time led to an  
323 increase in  $\text{CO}_2$  selectivity and a decrease in  $\text{CO}$  selectivity.

### 324 **Figure 11**

325 Figure 12 displays TPO curves of the coke deposited over Ni/Al<sub>2</sub>O<sub>3</sub> catalyst in the  
326 steam reforming of phenol when different amounts of catalyst are used at 750 °C for 60  
327 min. It can be observed that the amount of catalyst used does not affect significantly the  
328 nature of the coke deposited but it does the amount of coke deposited over the catalyst.  
329 All the TPO curves present a main peak at 500 °C with a shoulder at 400 °C which  
330 evidences that the coke deposited over the catalyst has a similar degree of graphitization  
331 and similar location over the catalyst. Furthermore, as the amount of catalyst (catalytic  
332 bed length) is increased, the amount of coke deposited on the catalyst decreases.  
333 Consequently, based on the evolution of phenol concentration with catalyst amount, the  
334 role of phenol should be noted as coke precursor by phenate species adsorbed as  
335 intermediates [35].

#### 336 **Figure 12**

#### 337 **4. Conclusion**

338 High carbon conversion and H<sub>2</sub> potential has been obtained in the steam reforming of  
339 phenol over Ni/Al<sub>2</sub>O<sub>3</sub> catalyst, reaching a value of 81 and 59 %, respectively, at 750 °C  
340 for a reaction time of 60 min and using 1.5 g of catalyst. The coke deposited over the  
341 catalyst is mainly of low degree of graphitization and its amount has been lower than 5  
342 % in the whole operating range studied.

343 An increase in temperature gives way to an increase in carbon conversion and H<sub>2</sub>  
344 potential due to the enhancement of phenol reforming reaction. Besides, coke  
345 gasification rate increases as temperature is increased, and the amount of coke deposited  
346 over the catalyst significantly decreases (from 4.6 % to 1.1 %) when temperature is  
347 increased from 650 to 800 °C. However, a high reforming temperature (800 °C) causes  
348 an increase in Ni crystal size and, therefore, catalyst deactivation by sintering.

349 It is concluded that an initial period of NiO reduction is required to activate the catalyst.  
350 Thus, an increase in time on stream increases the carbon conversion and H<sub>2</sub> potential  
351 until 60 min of time on stream, from which the catalyst activity is maintained constant.  
352 Regarding coke deposition, an increase in time on stream influences the amount of coke  
353 deposited but also the nature of the coke, whose amount and graphitization degree is  
354 higher as reaction time increases.

355 The amount of the catalyst used has great influence on phenol steam reforming, with  
356 carbon conversion increasing linearly, as well as H<sub>2</sub> potential, with the amount of  
357 catalyst used. However, phenol conversion seems to have a ceiling value in the steam  
358 reforming, whereas a further enhancement of water gas shift reaction is observed.

359

### 360 **Acknowledgments**

361 Maite Artetxe thanks the University of the Basque Country UPV/EHU for her post-  
362 graduate Grant (UPV/EHU 2013). We also acknowledge support from the UK  
363 Engineering & Physical Sciences Research Council through Supergen Bioenergy Grant  
364 EP/M013162/1.

365

366

367 **Reference List**

- 368 [1] Demirbas A. Biofuels sources, biofuel policy, biofuel economy and global biofuel  
369 projections. *Energy Convers Manage* 2008;49:2106-16.
- 370 [2] Vassilev SV, Vassileva CG, Vassilev VS. Advantages and disadvantages of composition  
371 and properties of biomass in comparison with coal: An overview. *Fuel* 2015;158:330-  
372 50.
- 373 [3] Shen Y, Yoshikawa K. Recent progresses in catalytic tar elimination during biomass  
374 gasification or pyrolysis-A review. *Renewable Sustainable Energy Rev* 2013;21:371-92.
- 375 [4] Li D, Tamura M, Nakagawa Y, Tomishige K. Metal catalysts for steam reforming of tar  
376 derived from the gasification of lignocellulosic biomass. *Bioresour Technol*  
377 2015;178:53-64.
- 378 [5] Asadullah M. Barriers of commercial power generation using biomass gasification gas: A  
379 review. *Renewable Sustainable Energy Rev* 2014;29:201-15.
- 380 [6] Heidenreich S, Foscolo PU. New concepts in biomass gasification. *Prog Energy Combust*  
381 *Sci* 2015;46:72-95.
- 382 [7] Choudhury HA, Chakma S, Moholkar VS. Chapter 14 - Biomass Gasification Integrated  
383 Fischer-Tropsch Synthesis: Perspectives, Opportunities and Challenges. In: Sukumaran  
384 APBS, editor. *Recent Advances in Thermo-Chemical Conversion of Biomass*. Boston:  
385 Elsevier; 2015. p. 383-435.
- 386 [8] Anis S, Zainal ZA. Tar reduction in biomass producer gas via mechanical, catalytic and  
387 thermal methods: A review. *Renewable Sustainable Energy Rev* 2011;15:2355-77.
- 388 [9] Asadullah M. Biomass gasification gas cleaning for downstream applications: A  
389 comparative critical review. *Renewable Sustainable Energy Rev* 2014;40:118-32.
- 390 [10] Devi L, Ptasiński KJ, Janssen FJJG. A review of the primary measures for tar elimination  
391 in biomass gasification processes. *Biomass Bioenergy* 2003;24:125-40.
- 392 [11] Chan FL, Tanksale A. Review of recent developments in Ni-based catalysts for biomass  
393 gasification. *Renewable Sustainable Energy Rev* 2014;38:428-38.
- 394 [12] Goransson K, Soderlind U, He J, Zhang W. Review of syngas production via biomass  
395 DFBGs. *Renewable Sustainable Energy Rev* 2011;15:482-92.
- 396 [13] Constantinou DA, Efstathiou AM. The steam reforming of phenol over natural calcite  
397 materials. *Catal Today* 2009;143:17-24.
- 398 [14] Devi L, Ptasiński KJ, Janssen FJJG, van Paasen SVB, Bergman PCA, Kiel JHA. Catalytic  
399 decomposition of biomass tars: use of dolomite and untreated olivine. *Renewable*  
400 *Energy* 2005;30:565-87.
- 401 [15] Erkiaga A, Lopez G, Amutio M, Bilbao J, Olazar M. Steam gasification of biomass in a  
402 conical spouted bed reactor with olivine and  $\gamma$ -alumina as primary catalysts. *Fuel*  
403 *Process Technol* 2013;116:292-9.
- 404 [16] Tuomi S, Kaisalo N, Simell P, Kurkela E. Effect of pressure on tar decomposition activity  
405 of different bed materials in biomass gasification conditions. *Fuel* 2015;158:293-305.

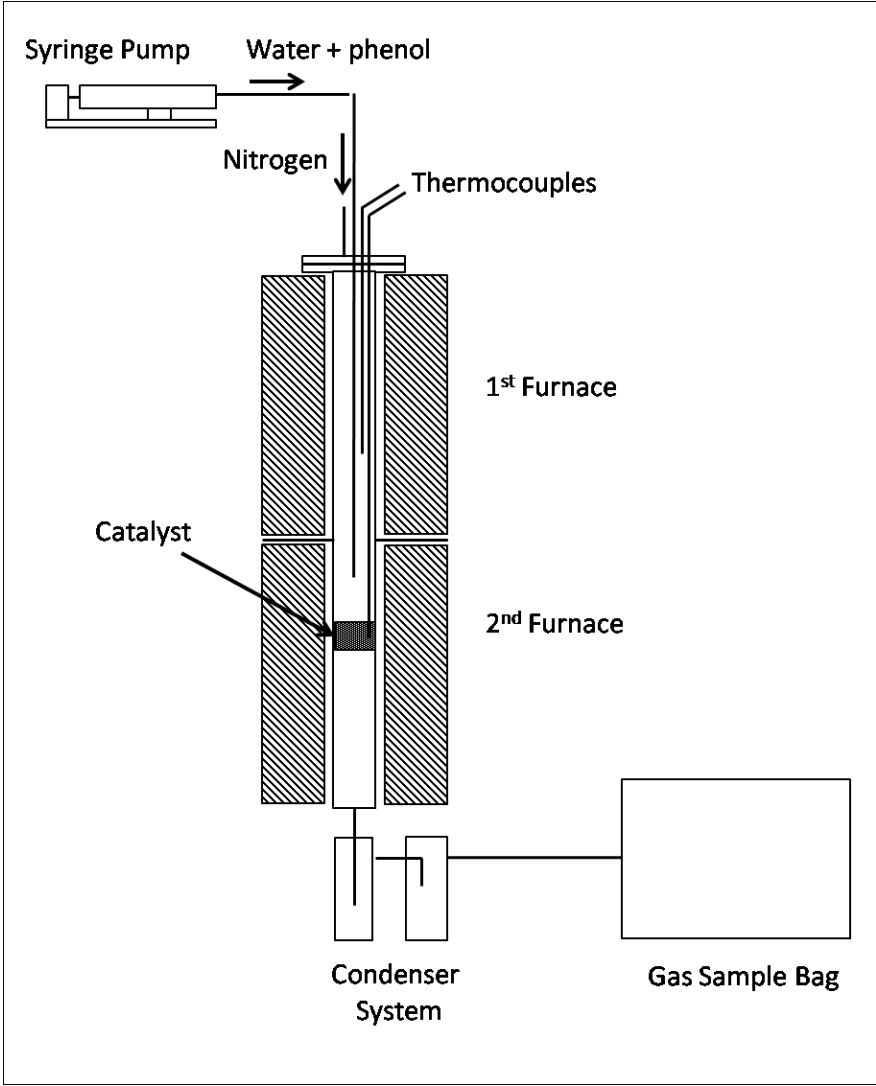
- 406 [17] Coll R, Salvado J, Farriol X, Montane D. Steam reforming model compounds of biomass  
407 gasification tars: conversion at different operating conditions and tendency towards coke  
408 formation. *Fuel Process Technol* 2001;74:19-31.
- 409 [18] Li C, Hirabayashi D, Suzuki K. Development of new nickel based catalyst for biomass tar  
410 steam reforming producing H<sub>2</sub>-rich syngas. *Fuel Process Technol* 2009;90:790-6.
- 411 [19] Zhang R, Wang H, Hou X. Catalytic reforming of toluene as tar model compound: Effect  
412 of Ce and Ce-Mg promoter using Ni/olivine catalyst. *Chemosphere* 2014;97:40-6.
- 413 [20] Park HJ, Park SH, Sohn JM, Park J, Jeon JK, Kim SS, et al. Steam reforming of biomass  
414 gasification tar using benzene as a model compound over various Ni supported metal  
415 oxide catalysts. *Bioresour Technol* 2010;101:S101-3.
- 416 [21] Koike M, Ishikawa C, Li D, Wang L, Nakagawa Y, Tomishige K. Catalytic performance  
417 of manganese-promoted nickel catalysts for the steam reforming of tar from biomass  
418 pyrolysis to synthesis gas. *Fuel* 2013;103:122-9.
- 419 [22] Bona S, Guillen P, Alcalde JG, Garcia L, Bilbao R. Toluene steam reforming using  
420 coprecipitated Ni/Al catalysts modified with lanthanum or cobalt. *Chem Eng Journal*  
421 2008;137:587-97.
- 422 [23] Laosiripojana N, Sutthisripok W, Charojrochkul S, Assabumrungrat S. Development of  
423 Ni-Fe bimetallic based catalysts for biomass tar cracking/reforming: Effects of catalyst  
424 support and co-fed reactants on tar conversion characteristics. *Fuel Process Technol*  
425 2014;127:26-32.
- 426 [24] Michel R, Lamacz A, Krzton A, Djéga-Mariadassou G, Burg P, Courson C, et al. Steam  
427 reforming of  $\alpha$ -methyl-naphthalene as a model tar compound over olivine and olivine  
428 supported nickel. *Fuel* 2013 Jul;109:653-60.
- 429 [25] Shen Y, Chen M, Sun T, Jia J. Catalytic reforming of pyrolysis tar over metallic nickel  
430 nanoparticles embedded in pyrochar. *Fuel* 2015;159:570-9.
- 431 [26] Ashok J, Kawi S. Steam reforming of toluene as a biomass tar model compound over  
432 CeO<sub>2</sub> promoted Ni/CaO-Al<sub>2</sub>O<sub>3</sub> catalytic systems. *Int J Hydrogen Energy*  
433 2013;38:13938-49.
- 434 [27] Wang S, Zhang F, Cai Q, Li X, Zhu L, Wang Q, et al. Catalytic steam reforming of bio-  
435 oil model compounds for hydrogen production over coal ash supported Ni catalyst. *Int J*  
436 *Hydrogen Energy* 2014;39:2018-25.
- 437 [28] Wang S, Cai Q, Zhang F, Li X, Zhang L, Luo Z. Hydrogen production via catalytic  
438 reforming of the bio-oil model compounds: Acetic acid, phenol and hydroxyacetone. *Int*  
439 *J Hydrogen Energy* 2014;39:18675-87.
- 440 [29] Wu C, Williams PT. Hydrogen production by steam gasification of polypropylene with  
441 various nickel catalysts. *Appl Catal, B* 2009;87:152-61.
- 442 [30] Efica CE, Wu C, Williams PT. Syngas production from pyrolysis-catalytic steam  
443 reforming of waste biomass in a continuous screw kiln reactor. *J Anal Appl Pyrolysis*  
444 2012;95:87-94.
- 445 [31] Polychronopoulou K, Bakandritsos A, Tzitzios V, Fierro JLG, Efstathiou AM.  
446 Absorption-enhanced reforming of phenol by steam over supported Fe catalysts. *J Catal*  
447 2006;241:132-48.

- 448 [32] Matas Guell B, Babich IV, Lefferts L, Seshan K. Steam reforming of phenol over Ni-  
449 based catalysts - A comparative study. *Appl Catal, B* 2011;106:280-6.
- 450 [33] Wu C, Williams PT. Investigation of coke formation on Ni-Mg-Al catalyst for hydrogen  
451 production from the catalytic steam pyrolysis-gasification of polypropylene. *Appl Catal,*  
452 *B* 2010;96:198-207.
- 453 [34] Vicente J, Montero C, Ereña J, Azkoiti MJ, Bilbao J, Gayubo AG. Coke deactivation of  
454 Ni and Co catalysts in ethanol steam reforming at mild temperatures in a fluidized bed  
455 reactor. *Int J Hydrogen Energy* 2014;39:12586-96.
- 456 [35] Garbarino G, Sanchez Escribano V, Finocchio E, Busca G. Steam reforming of phenol-  
457 ethanol mixture over 5% Ni/Al<sub>2</sub>O<sub>3</sub>. *Appl Catal, B* 2012;113-114:281-9.
- 458 [36] Remiro A, Valle B, Aguayo AT, Bilbao J, Gayubo AG. Operating conditions for  
459 attenuating Ni/La<sub>2</sub>O<sub>3</sub>-Al<sub>2</sub>O<sub>3</sub> catalyst deactivation in the steam reforming of bio-oil  
460 aqueous fraction. *Fuel Process Technol* 2013;115:222-32.
- 461 [37] Clause O, Gazzano M, Trifiro F, Vaccari A, Zatorski L. Preparation and thermal  
462 reactivity of nickel/chromium and nickel/aluminium hydrotalcite-type precursors. *Appl*  
463 *Catal* 1991;73:217-36.
- 464 [38] Swierczynski D, Courson C, Kiennemann A. Study of steam reforming of toluene used as  
465 model compound of tar produced by biomass gasification. *Chem Eng Process Process*  
466 *Intensif* 2008;47:508-13.
- 467
- 468

469 **Figure captions**

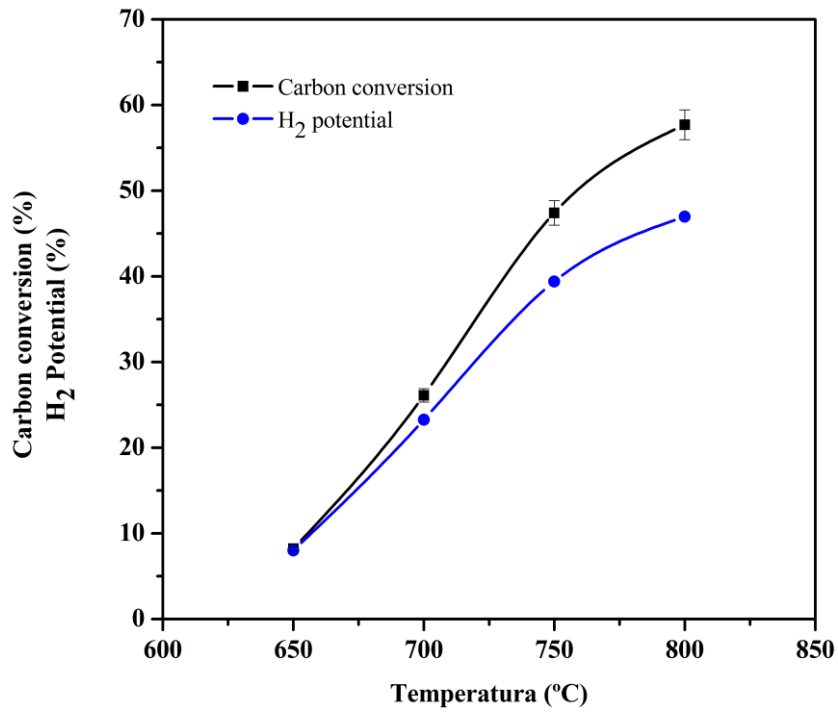
- 470 Figure 1. Experimental equipment used for steam reforming of phenol.
- 471 Figure 2. Effect of temperature on carbon conversion and H<sub>2</sub> potential (40 min; 1 g of  
472 catalyst).
- 473 Figure 3. Effect of temperature on gas compounds yield (40 min; 1 g of catalyst).
- 474 Figure 4. DTG-TPO curves of the coke deposited over the catalyst used at different  
475 temperatures (40 min; 1 g of catalyst).
- 476 Figure 5. SEM imagines of the fresh catalyst (a) and used catalyst at 650 (b), 750 (c)  
477 and 800 °C (d) (40 min; 1 g of catalyst).
- 478 Figure 6. Effect of reaction time on carbon conversion and H<sub>2</sub> potential (750 °C; 1 g  
479 of catalyst).
- 480 Figure 7. Effect of reaction time on gas compounds yield (750 °C; 1 g of catalyst).
- 481 Figure 8. DTG-TPO curves of the coke deposited over the catalyst used for different  
482 reaction times (750 °C; 1 g of catalyst).
- 483 Figure 9. SEM imagines of the fresh catalyst (a) and used catalyst for 40 (b), 60 (c)  
484 and 80 (d) min (750 °C; 1 g of catalyst).
- 485 Figure 10. Effect of catalyst amount on carbon conversion and H<sub>2</sub> potential (750 °C; 60  
486 min).
- 487 Figure 11. Effect of catalyst amount on gas compounds yield (750 °C; 60 min).
- 488 Figure 12. DTG-TPO curves of the coke deposited over the catalyst used for different  
489 catalyst amounts (750 °C; 60 min).

490



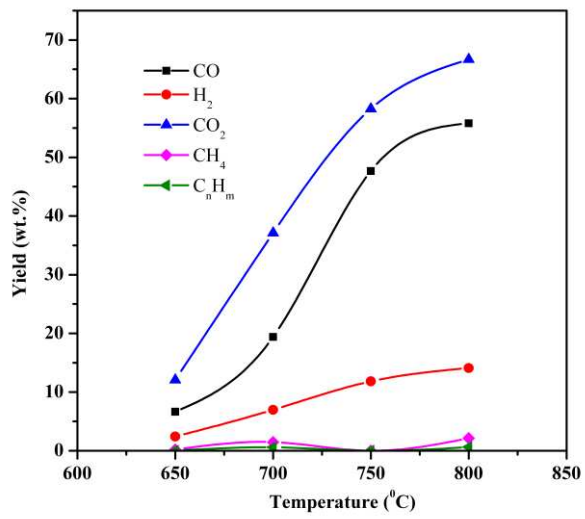
491

492



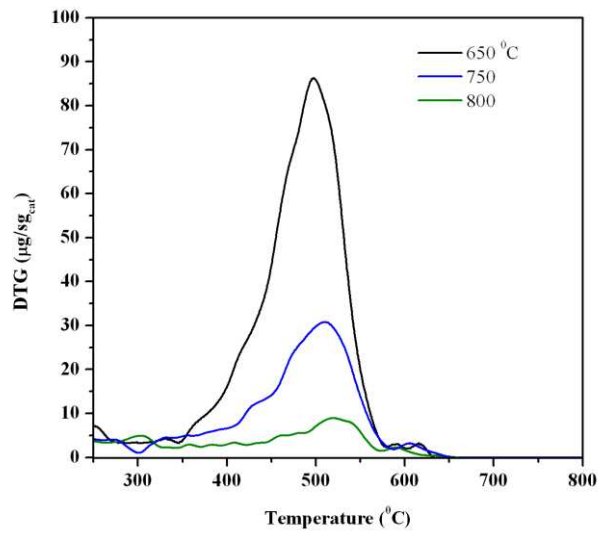
493

494



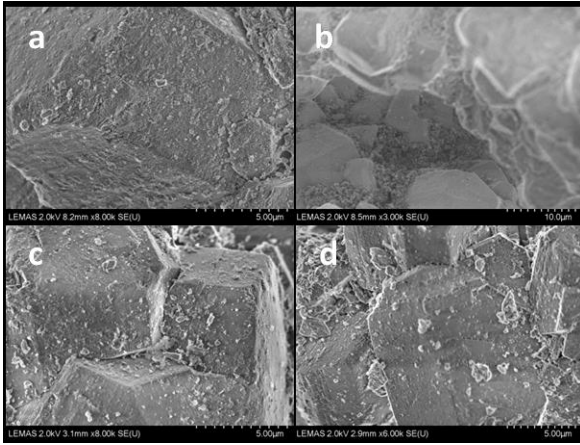
495

496



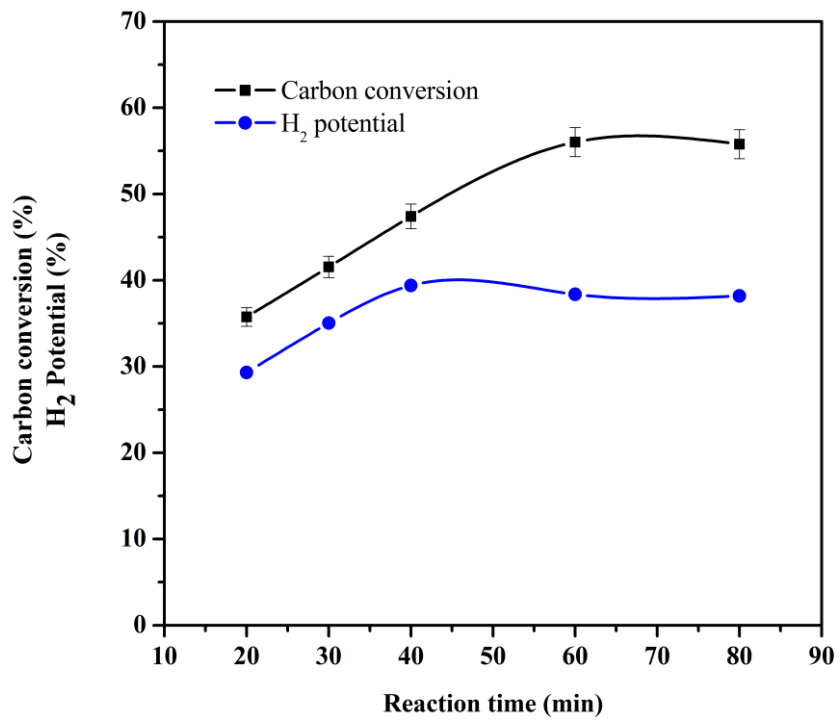
497

498



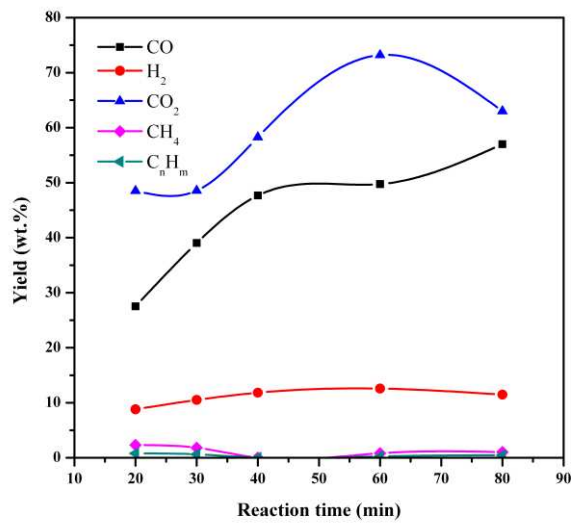
499

500



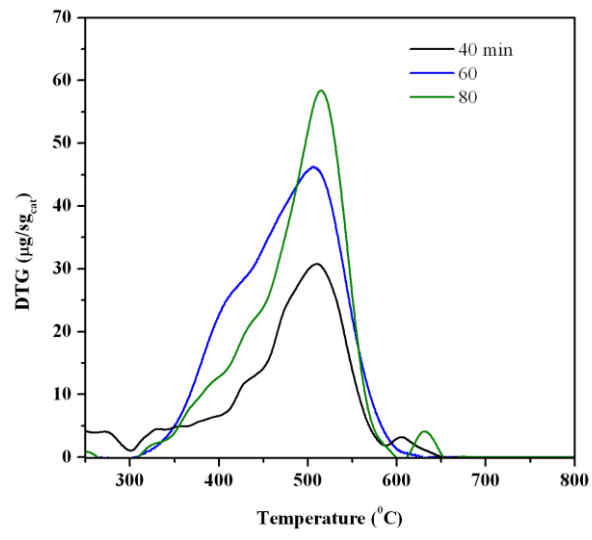
501

502



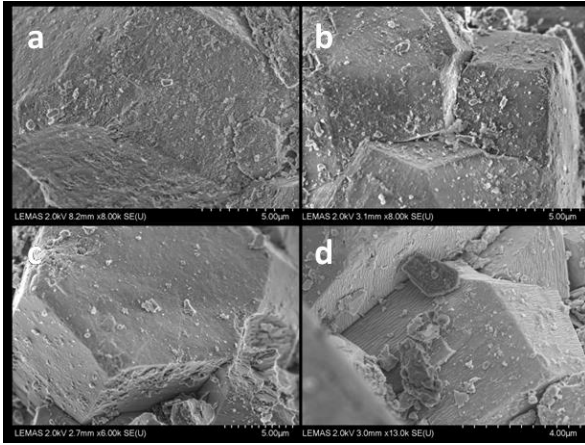
503

504



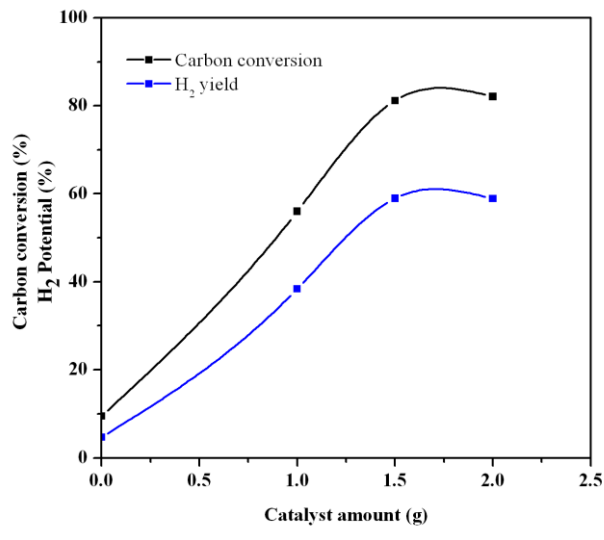
505

506



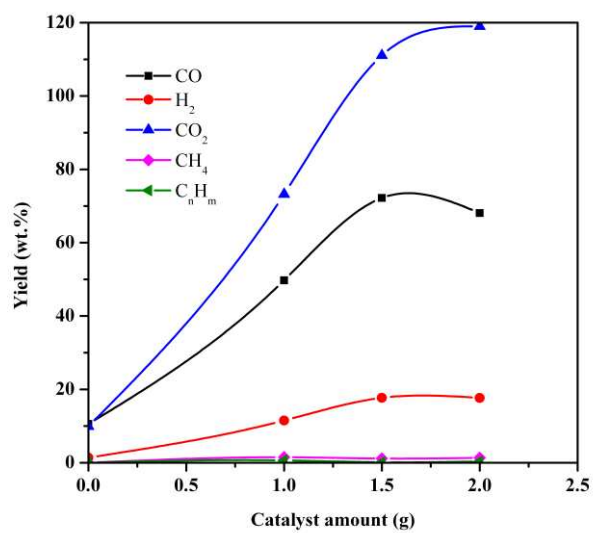
507

508



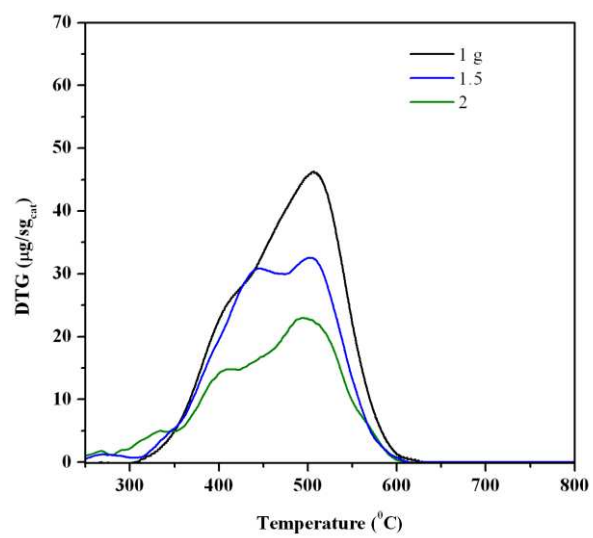
509

510



511

512



513

514

515